Lawrence Berkeley Laboratory
UNIVERSITY OF CALIFORNIA

Accelerator & Fusion
Research Division

Submitted to the Journal of Plasma Physics

EXPERIMENTAL RESULTS ON TRAPPING A GUN PLASMA IN A TOROIDAL MAGNETIC CUSP EXPERIMENT

P.A. Pincosy, B.R. Myers, M.A. Levine,
B. Feinberg, R.A. Niland, and L. Soroka

November 1983

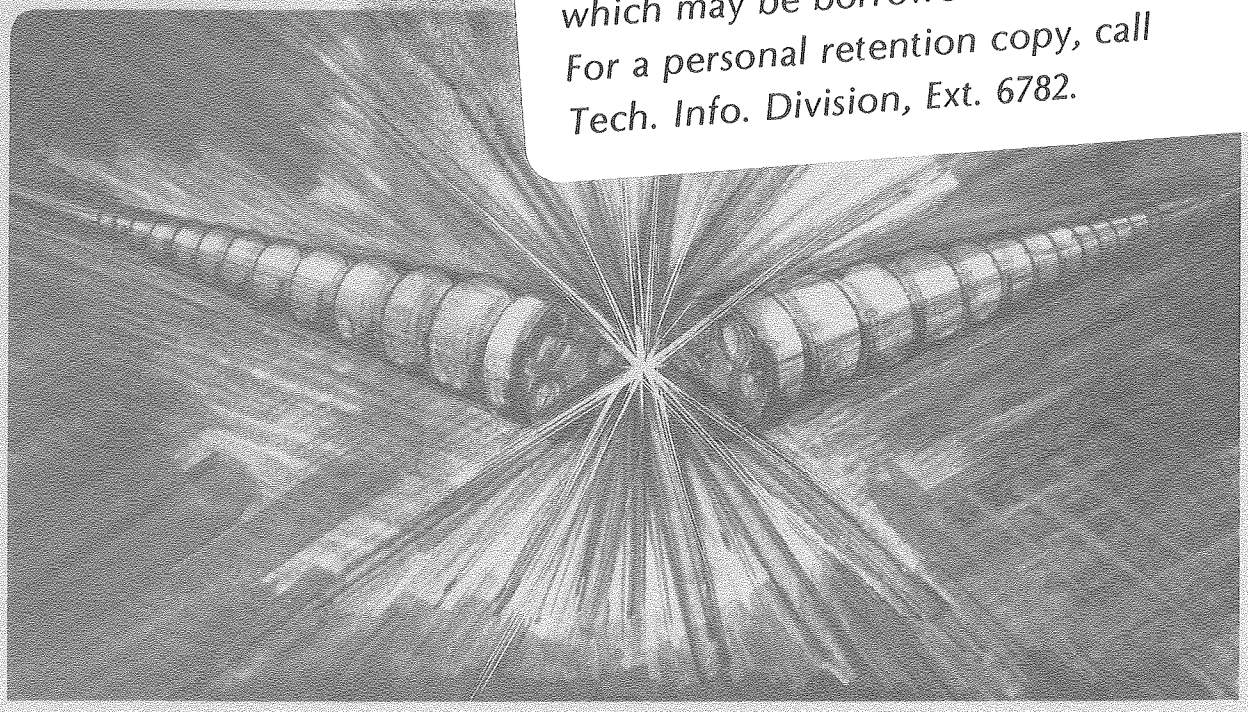

Prepared for the U.S. Department of Energy under Contract DE-AC03-76SF00098

DISCLAIMER

EXPERIMENTAL RESULTS ON TRAPPING A GUN PLASMA IN A TOROIDAL MAGNETIC CUSP EXPERIMENT

P. A. Pincosy, B. R. Myers[a], M. A. Levine,
B. Feinberg, R. A. Niland[b], and L. Soroka

Lawrence Berkeley Laboratory
University of California
Berkeley, California 94720

ABSTRACT

A start-up scheme for producing a plasma in the bi-cusp field configuration of a toroidal magnetic cusp experiment (TORMAC) which involves the radial injection and trapping of a toroidal gun plasma is described. The poloidal field of the external cusp coils acts as a barrier to the outward travel of the plasma ring. Interferometry and magnetic probe measurements were used to observe the stopping of the expanding plasma ring which has a velocity of 17 cm/μsec. Once stopped, the fields are arranged to hold the plasma in a magnetic well. A well-defined outer boundary remained stationary during the 20 μsec of the interferometry measurement. The indications of the particle flux distribution emanating from the cusp are that a

---

* This work was supported by the Fusion Energy Division of the U.S. Department of Energy under Contract No. DE-AC03-76SF00098.

a Current Address: Lawrence Livermore National Laboratory, Livermore CA.

b Current Address: School of Physics, University of Sydney, NSW, Australia.

sheath exists having a width of 1 to 1.5 ion gyro radii in the poloidial field. This translates to a narrow outer boundary and a broad inner boundary based on the gradient of the poloidial field at the two radial positions. Measurements of Thomson scattering and interferometry give a T_e of 15 eV, a 15 μsec density decay time, and a 5 μsec energy decay time. These results show that this injection and trapping method is successful, and thus a higher gun plasma energy combined with a flux conserving barrier may lead to higher temperatures for testing containment in TORMAC.

I. INTRODUCTION

Among the possible magnetic confinement schemes envisioned for fusion, the cusp configuration has the unique feature of being stable to magneto-hydrodynamic (MHD) disturbances at high β (Berkowitz et al., 1958, Haines, 1977 and Spaulding, 1971). As Levine and Boozer (1973), have shown, there exists a canonical invariant for cusps which led them to propose a scheme for particle confinement meeting the Lawson criterion (Lawson, 1957). One problem in attaining the conditions for cusp confinement is the difficulty of producing the necessary plasma and field configuration.

Spalding (1971) in his review of cusp confinement notes that there is a major experimental problem in establishing a plasma with properties approaching the free boundary equilibrium required by theory. Previous experiments used in-situ ionization and compression, (Watteau, 1961 and Brown et al., 1982) shock heating (Spalding et al., 1969) or gun injection (Osher, 1962). With the exception of the Centaur experiment (Spalding et al., 1969), the

technique of in-situ ionization, compression and shock heating has probably failed to attain collisionless conditions. The addition of a "stuffing" field as desired for testing the theory of Levine and Boozer, renders compression or shocking of the plasma to a collisionless condition even more difficult (Brown et al., 1982 and Vella et al., 1979). Fortunately, plasma guns have proved to be a more effective method of transferring the appropriate energy to a plasma.

In a series of injection experiments, Osher (1962) used a coaxial gun which fired into a static cusp. The electrons are considered to be trapped in an adiabatic cusped field. These experiments produced high temperature electrons and hot ions but did not attain the required high beta free boundary conditions. Evidence produced by X-ray measurements for "strong cooperative effects" is cited as one reason. A different plasma gun configuration and injection technique was proposed in order to avoid such effects. This gun has similarities to inverse pinches which are shown (Vlases, 1967) to operate stably.

A toroidally symmetric plasma gun with annular electrodes (Fig. 1) was constructed and tested (Myers et al., 1979). The important features are discussed. A plasma ring produced by the gun is observed to expand in major radius along with a small trailing plasma density. The acceleration of this plasma ring is aided by a resident torodial bias field. In addition, the application of a poloidal bias field (plasma gun poloidal field windings of Fig. 1) induces a toroidal current in the plasma ring as it is pushed outward. This toroidal current is designed to close poloidal field

lines in the plasma core and to "stabilize" the gun plasma in a "tokamak-like" configuration.

This paper presents the results of injecting the plasma ring into a quasi-static cusp. Most of the results were obtained with a hydrogen plasma ring velocity of 17×10^6 cm/sec (150 eV). A few measurements were made with an upgraded plasma gun design, giving a velocity of 43×10^6 cm/sec (1000 eV). A stuffed toroidal bi-cusp (Gallagher et al., 1970) was chosen for injection and trapping of the plasma. The bi-cusp is a two-pole toroidally symmetric line cusp which combines toroidal and poloidal magnetic fields to create a minimum-B well.

The scheme for the experiment involves the transport of the MHD "stable" gun plasma into the bi-cusp fields. The stability is ensured because the transit time of the gun plasma is short. The increasing poloidal field of the external cusp coils acts as a barrier to the radially outward travel of the plasma ring. This barrier is needed to stop the outward motion on a time scale sufficiently short for the compression and thermalization of the plasma. A zero order estimate of the final conditions of the plasma in the equilibrium well is made by assuming the gun plasma has undergone an adiabatic compression by the action of the barrier and an expansion to the final pressure balance. If the stopping time scale is sufficiently rapid, any resultant thermalization could be modeled by using the MHD shock relations followed by an adiabatic expansion to a pressure equilibrium. Further description of the equilibrium plasma configuration is modeled by simulating a $\beta=1$ plasma with skin currents.

In this paper it is reported that the gun plasma does not pass through the poloidal field but settles in the field well with a sheath boundary.

II. ASPECTS OF TRAPPING

The bi-cusp configuration for TORMAC consists of poloidal cusp-field confinement on the outer radius of a torus and toroidal field confinement on the inner side of the plasma torus. These features provide the good curvature required for MHD stable confinement of a high-β plasma. The coil structures shown in Fig. 1 provide the vacuum fields whose poloidal flux lines are illustrated in Fig. 2(a). Contours of constant field magnitude which include both the toroidal and poloidal field components and which show the minimum-B well are illustrated in Fig. 2(b). Looking along a radius at the mid-plane ($z = o$) the intensity of the vacuum poloidal field B_p (see Fig. 3) is small (< 100 gauss) for $R < 26$ cm and $B_p \propto I_c(R-26)$ for $R > 26$ cm, where I_c is the coil current. The toroidal field falls off as $1/R$ from the center conductors and the plasma produced by the gun flows freely through the toroidal field except for the mild gradient forces. However, the plasma interacts strongly with the poloidal magnetic field.

The overall process is considered in three steps by proposing simple models to describe the plasma ring injection and stopping, the thermalization of the plasma ring, and finally the equilibrium state and configuration. For the thermalization, the maximum possible temperature is considered and then a more realistic model is presented.

possible temperature is considered and then a more realistic model is presented.

The plasma ejected from the gun is toroidally continuous (Myers et al., 1979) allowing the induction of a toroidal current by the poloidal field in the interacting boundary. Thus, the decelerating force on the outgoing plasma is the poloidal magnetic pressure integrated over the interacting boundary. If a flux conserving metal hoop were placed at some major radius, then the poloidal flux trapped between the hoop and the plasma ring would cause the field, and thus the stopping force, to rise enough to stop the plasma. For the experiments having a plasma ring velocity of 17 cm/μsec, the flux conserving ring is not necessary because the poloidal field alone is sufficiently strong. The stopping, of course, always requires that the plasma ring be toroidally connected. It is thus appropriate to require that the plasma skin depth be nowhere more than the minor diameter. Typically, the skin depth for a 10 eV plasma (about the electron temperature of the plasma ring) stopped in 0.2 μsec is 0.02 cm. A first order estimate of the stopping position can be made by considering the momentum balance,

$$\int NmdV = -\int F_d dt \qquad (1)$$

where N is the total number of particles of mass m with directed velocity V and F_d is the decelerating force. Supposing the B_p field gradient in the plasma has a scale length small compared to the radial thickness of the plasma ring, the induced force

decelerating the plasma can be written as follows,

$$F_d = \frac{1}{4} aRB_p^2, \qquad (2)$$

here the poloidal field, B_p, is assumed to vary linearly with R and is applied across a plasma ring width. Integrating over the distance traveled and applying the limits of the velocity which go from the initial value, V_p, to 0 as R goes from R_o to R_2, the radius of deepest penetration, R_2, is given by the following expression:

$$(R_2 - R_o)^4 + \frac{4}{3} R_o (R_2 - R_o)^3 - \frac{8mN}{a} \frac{(R_e - R_o)^2}{B_{p_e}^2} V_p^2 = 0 , \qquad (3)$$

where R_o is the radius at which B_p is zero and R_e is a radius exterior to any plasma travel at which $B_p = B_{p_e}$. Using this relationship to predict the stopping position of the plasma ring requires the knowledge of the total particle number N being stopped, the plasma ring velocity V_p and the plasma width, a, at the stopping point. Measured values of $N \simeq 4 \times 10^{18}$ particles, and $V_p = 17$ cm/μsec can be used directly. Measurements also show that the plasma ring radial dimension of 5 cm does not increase as the ring increases in major radius, but the lateral expansion was not measured. At the gun, this width is 3 cm but the ring can spread laterally. The transit time from the gun to the stopping point is measured to be 0.9 μsec so that the final width would be a = 11.6 cm assuming a free expansion at the acoustic velocity based on an

electron temperature of 10 eV. Taking the best linear approximation of B_p where R_e is chosen with B_p = 3.0 kG (see Fig. 3), the stopping position, R_2 is calculated for three lateral widths of the plasma, 3 cm, 6 cm and 12 cm. The stopping positions (Table I) are respectively 39.4, 37.2 and 35.4 cm.

For the case where V_p = 43 cm/μsec, B_{p_e} must be 9.5 kG in order to stop the plasma at R_2 = 38 cm just inside the magnetic field coils if the plasma width was 3 cm.

The most basic consideration which gives an upper limit on the maximum final temperature is the ideal case when all the directed energy is transformed into thermal energy through an adiabatic expansion to the final equilibrium. The gun plasma particle energy,

$$E_{gun} = \frac{m_i}{2} V_p^2, \tag{4}$$

is 150 eV for the case where the ring plasma velocity, V_p = 17 cm/μsec. The equivalent thermal energy content divided between electrons and ions is 3 kT_i, where $T_i = T_e$. Assuming the thermal plasma then expands adiabatically to equilibrium and excludes the poloidal field, $k(T_i + T_e)$ of work is lost in the expansion of the plasma boundary. Equating the thermal energy plus the expansion energy to the gun plasma energy E_{gun} indicates a final $T_i = T_e$ = 1/5 E_{gun} = 30 eV. This is the maximum possible final temperature.

A more sophisticated model would suppose the plasma undergoes thermalization by a shock (Tidman and Krall, 1971). The time scale of deceleration, $_d$ is considered shorter than an Alfven wave

transit time, τ_t radially across the plasma ring. That is

$$\tau_d < \tau_t = 2a/V_A \simeq 0.4\ \mu\text{sec} \tag{5}$$

where V_A is estimated to be 12 cm/μsec. From the de Hoffmann-Teller (1960) relationships derived for a perpendicular magnetic shock, the following expressions across a shock are related to the initial plasma beta, β_1, and the laboratory plasma Mach. No., M_p.

$$M_1 = f(M_1) = \left\{\frac{1}{7}\left[8M_1M_p + \frac{5}{2}(\beta_1 + 1) + S_q\right]\right\}^{1/2} \tag{6}$$

$$\eta = \frac{n_1}{n_2} = \frac{v_2}{v_1} = \frac{B_1}{B_2} = \frac{1}{8M_1^2}\left\{\frac{5}{2}\beta_1 + 1 + M_1^2\right\} + S_q \tag{7}$$

$$\beta_2 = \frac{1}{5}\left\{\eta\left[5\beta_1 + 4 + 2M_1^2(1 - \eta^2)\right] - 4\right\} \tag{8}$$

$$\frac{T_2}{T_1} = \beta_2/(\beta_1\eta) \tag{9}$$

where

$$S_q = \left\{\left[\frac{5}{2}(\beta_1 + 1) + M_1^2\right]^2 + 8M_1^2\right\}^{1/2} \tag{10}$$

1 and 2 denote the upstream and downstream condition for shock fixed coordinates where M is the Alfven Mach No., n is the local number density, T is the temperature, and $\beta = 8\pi nkT/B^2$.

An estimate of the initial value of β is obtained by assuming that the toroidal magnetic field, imbedded in the plasma, has the

value of the vacuum field at the stopping position and that the plasma electron temperature is 10 eV. The vacuum toroidal field is chosen because the plasma is formed in the strong toroidal field region and the plasma expands to keep pressure balance as it moves radially outward. Thus, the imbedded toroidal field is the value which determines the Alfven wave speed. The assumed temperature has only a small influence on the final condition because the thermal energy density of the plasma is much less than the directed energy density.

The final equilibrium condition of the post-shocked plasma is evaluated by using the adiabatic relationships for a frozen field (Jackson, 1962) expansion to a pressure equilibrium based on the value of the vacuum magnetic field at the position where an outer boundary is experimentally observed. The relationships are as follows:

$$\text{Expansion:} \quad \frac{T_f}{n_f^{\gamma-1}} = \frac{T_2}{n_2^{\gamma-1}} \tag{11}$$

$$\text{Frozen Field:} \quad \frac{B_f}{B_2} = \frac{n_f}{n_2}\,\frac{R_f}{R_2} \tag{12}$$

where R_f is the mean radial position of the equilibrium plasma and

R_2 is the outer stopping position of the plasma.

Equilibrium Pressure Balance:

$$n_f k T_f + \frac{B_f^2}{8\pi} = \frac{B_o^2}{8\pi} \tag{13}$$

Some estimates of the final plasma conditions are made with this model using some of the measured initial conditions and assuming a range of values for the major unknown initial conditions. The initial electron temperature T_1 is assumed to be 10 eV whereas the density n_1 is chosen to have three possible values each concurring with a lateral dimension, a, such that the line-of-sight nl = 3 x 10^{15} cm^{-2} as was measured at R = 34 cm for the plasma ring velocity V_p = 17 cm/μsec. The imbedded toroidal field value at the stopping point, R_2 = 34 cm is estimated to be B_1 = 1.7 kG. The final equilibrium radius R_f = 28 cm was based on the centroid of the equilibrium plasma cross-section as measured. At this location the external equilibrium field B_e = 2 kG. Table 1 shows the initial and final conditions for three densities relating to plasma ring widths of 3 cm, 6 cm and 12 cm.

Considering that the plasma velocity is 17 cm/μsec and that the stopping time is about 0.3 μsec, or not much less than the Alfven wave transit time, neither model accounts for the true experimental conditions and, thus, they can only be considered as guides to the equilibrium conditions.

The models have so far addressed the transition of the plasma

state from the ring to the equilibrium. In order to predict the plasma equilibrium shape, a $\beta = 1$ plasma (excludes poloidal field) is simulated (Feinberg et al., 1983) by a set of closed toroidal current loops on the plasma boundary. The computer code adjusts the currents of these loops and their positions to find a solution which has a constant pressure and a constant flux on the boundary. It is primarily the plasma pressure which determines the size of the plasma volume. Since the pressure is not known, the imposed condition for determining the pressure on the boundary is the radial location of the outer boundary as measured experimentally. The pressure is varied until the outer boundary corresponds to the experimentally measured boundary. The flux value on the boundary is obtained by matching the location of the inner boundary to the location of the experimentally measured inner boundary. This is somewhat arbitrary in view of the large width of the inner boundary. The plasma shape as denoted by the Δ's in Fig. 4 is an equilibrium solution. The field is everywhere modified so that the field lines extending from the equilibrium plasma location to the outside of the coil structure of the torus are as shown in Fig. 5(a) compared to those vacuum fields of Fig. 5(b).

The experimental plasma is not a $\beta = 1$ plasma. Provided that the field on the inner boundary is purely toroidal and that the field in the plasma is purely toroidal, the spatial dependence between the external poloidal and toroidal field for pressure balance is independent of the internal toroidal field. That is, the toroidal beta of the plasma does not affect the shape since the functional dependence on R of the poloidal field, B_p, is the same

for any β_T as is seen in the expression derived from the pressure balance across the boundary.

$$P_T + \frac{B_i^2}{8\pi} = \frac{B_T^2 + B_P^2}{8\pi} \tag{14}$$

where B_i is the internal toroidal magnetic field, and B_T and B_p are the external toroidal and poloidal field components. Defining the toroidal beta at the inner-radial boundary by $\beta_T = P_T/(B_{T_o}^2/8\pi)$ and assuming the toroidal fields are inversely proportional to the radius, the above relationship becomes

$$\beta_T + \left(\frac{B_{io}^2}{B_{T_o}^2} - 1\right)\frac{R_o^2}{R^2} = \frac{B_P^2}{B_{T_o}^2} \tag{15}$$

At the inner radial boundary, the pressure balance is

$$P_T + \frac{B_{io}^2}{8\pi} = \frac{B_{T_o}^2}{8\pi} \qquad \text{or} \qquad \beta_T + B_{i_o}^2/B_{T_o}^2 = 1 \tag{16}$$

Eliminating B_{io}^2

$$\frac{B_P^2}{B_{T_o}^2} = \beta_T\left(1 - \frac{R_o^2}{R^2}\right) \tag{17}$$

Therefore, whether β_T is unity or not, the relationship of the boundary poloidal field to the radial position is only one of a scale factor and not of geometry. For the experimental case this is

approximately true since $B_p << B_T$ at the inner boundary (see Fig. 3 at R ≃ 25 cm).

With these models under consideration the experimental data will indicate what validity they have in describing the process the plasma ring undergoes to arrive at the equilibrium condition.

III. EXPERIMENTAL RESULTS

A. Apparatus

The experimental apparatus includes the bi-cusp windings in addition to the parts described previously (Myers et al., 1979): that is, the gas valve, the plasma gun plates and the toroidal field windings (Fig. 1). The radially symmetric gas valve (Myers et al., 1981) directs the flow toward the inner edge of the high voltage gun plate about 150 μsec before applying the voltage. The gun plates have an inner and outer radius of 8.5 and 19 cm, respectively, with a spacing of 3 cm between them. A 2.1 μF capacitor charged to 50 kV is connected across the plates by means of a spark gap switch. The gas breaks down in the resulting electric field and J x B forces on the plasma ring accelerate it radially outward. This acceleration is enhanced by the presence of the toroidal magnetic field when this field is in the same direction as that resulting from the capacitor discharge. The total number of particles is regulated by the filling pressure of the plenum in the gas valve, and in practice can be varied over the range of 10^{18} to 10^{19} particles (hydrogen). The dynamics at the gun are such that the total kinetic energy of the plasma (~200 Joules) remains roughly constant with different fill pressures. The plasma emerging from the 40 cm diameter gun has

a radial thickness of about 7 centimeters (300 ns, Fig. 6) that remains approximately constant as the major radius of the ring increases. At least 60 percent of the accelerated particles are contained in this initial "ring" (Fig. 7). These experiments were done without the poloidal bi-cusp windings. Upon adding the poloidal windings, some magnetic field is present between the gun plates even though, as noted previously, a field bucking coil (Fig. 4) was added to reduce this component. With these poloidal field windings, the plasma ring gun velocity was 17 cm/μsec, not as high as that measured (25 cm/μsec) without the poloidal field.

The influence of poloidal field between the plates was investigated briefly by imposing a similar poloidal field through the use of the gun poloidal field windings (see Fig. 1). It suffices to note that as the flux enclosed by the plasma increases, there is a point at which no plasma ring was ejected by the gun. The essential concern is that the plasma gun effectively eject a symmetrical plasma ring for injection into the containment field geometry.

The plasma gun poloidal field windings were installed for the option of inducing a toroidal current in the plasma ring as it is ejected. When the gun was operated with only the toroidal coils, a toroidal current of a few kiloamperes was measured with an applied poloidal field between the plates.

Even with the poloidal bucking coils, some poloidal field is resident between the plates and some induced toroidal current must have resulted. This current should not have played any role in the trapping process. Once the conditions were set so that the gun

produced a good plasma ring, experiments were made on the stopping of the ring and the formation of the stationary equilibrium.

An improved gun was tested for a few discharges. The upgrade consisted of reducing the circuit inductance by close coupling a 6.8 μf capacitor to the gun plates. The resultant circuit rise time was decreased from 0.6 μsec to 0.3 μsec.

The toroidal and bi-cusp poloidal windings are a series-parallel combination which are supplied by a capacitance of 1.2 F and voltages (V) up to 400 V. The resultant center-post axial current

$$I_{max} = V \times 10^3 \text{ amps} \qquad (18)$$

has a rise time of 5 msec. The bi-cusp windings in principle carry equal currents, whereas in practice there are some differences due to circuit imbalances. The six outermost windings at the same radius are located as shown in Fig. 2(a). The side windings with currents in the opposite direction to the outer ones are also shown in Fig. 2(a).

B. Diagnostic Measurements

The diagnostics used for these experiments are located as indicated in Fig. 4(a). The magnetic probe located at R = 37 cm was oriented to measure the poloidal field perturbation caused by the current induced in the plasma ring during deceleration.

The time varying axial line density is measured by using a stabilized Michelson interferometer (Myers et al., 1979) (Fig. 6). The interferometer can be moved radially from discharge to

discharge. Stabilization by an active feed-back circuit keeps the measurement sensitivity at the maximum, half way between constructive interference and destructive interference. The line density is given by:

$$\int n_e \, dl \; (cm^{-2}) = 2.8 \times 10^{16} \sin^{-1} (\Delta\varepsilon/V_0) \qquad (19)$$

where $\Delta\varepsilon$ is the measured voltage change and V_0 is half the total peak-to-peak voltage swing for a complete fringe. The interferometer measures the line integral of the electron density along the laser beam through the plasma with a minimum measurement sensitivity of about 10^{14} cm^{-2}.

A ruby laser used for the Thomson scattering measurement is aligned as indicated in Fig. 4(a) with a focal volume 3 mm in diameter and 4 cm long. A "notched" triple-grating polychromater (Greenwald and Smith, 1977) is used to spectrally analyze the scattered light. A three-lens system gathers this light from a 4 mm diameter by 4 cm long volume and images it onto the slit of a polychromater. Four channels of the polychromater are used, each having a 3 nm width with the first centered at 4.5 nm from the laser line center and the others spaced at 4.5 nm intervals. Care is taken not to include any part of the gun in the collection cone to minimize plasma light; also a viewing dump is included.

Magnetic field probes in a glass envelope are used to measure field perturbations caused by the plasma. The signals are integrated with a passive network having a time constant of 5 μsec and the estimated signal response time for the probe is a few nsec.

After a search with a Faraday Cup to find where the flux of particles emanates from the plasma, the cup was displaced along the line indicated in Fig. 5. In order to avoid saturation, the cup was also moved out to the lowest field region accessible, thus, giving a minimum flux of particles. The magnetic field at the measurement positions is calculated to be 100 G compared to 6000 G at the cusps. The line of measurement was oriented as closely as possible perpendicular to the field lines along a constant field magnitude contour.

C. Gun Plasma Condition

The velocity of the plasma ring is determined by measuring the plasma arrival time at the interferometer (Fig. 8) test beam for various radii on a discharge to discharge basis. The observed jitter is minimized by referring the arrival time to a peak of emitted plasma light gathered at a fixed radial position. The least-squares fit of the data does not include the five measurements closest to the position where the plasma ring stops moving. The spread of these five points indicates that the plasma ring is decelerated in a relatively short distance (a few centimeters). For the experiments reported herein, the expanding hydrogen plasma ring has a particle velocity of 17 cm/μsec, and particle energy of 150 eV. The improved gun produces a plasma ring having a particle velocity of 43 cm/μsec or a directed energy of 950 eV.

As the plasma ring moves radially outward, the passage duration (0.25 μsec) is observed to be constant with radius. From the measured velocity and passage duration, the estimated radial

thickness of the plasma ring is 5 cm. The average particle line density during the ring passage is 3×10^{15} cm^{-2}. Integrating the measured line density over the burst-time and assuming that all the particles have the same velocity, the total number of particles is about 4×10^{18} and the energy is estimated to be 90 joules

$$N_p = 2\pi R\, V_p \int_0^{t_p} \langle n_e \; 1_p \rangle dt \quad \text{and} \quad E_p = \frac{1}{2} M N_p V_p^2 \tag{20}$$

Also, toroidal symmetry is assumed and the burst is integrated up to $t_p = 0.5$ μsec at which time the tail of particles from the gun (see typical burst of Fig. 6 and Fig. 8) generally was a relatively low value of line density (less than 0.2 of peak density).

The electron temperature in the plasma ring leaving the gun was not measured except on one occasion. For that one discharge the Thomson scattering data gave 10 eV. However, as already noted, it is not crucial to know the particle temperatures since that energy is small compared to the directed energy in the moving ring.

D. Limit of Plasma Ring Expansion

The toroidal vacuum field decreases with radius, and beyond the radius of 25 cm the poloidal field increases (Fig. 3). The poloidal magnetic field probe placed at a radius of 37 cm measures a field perturbation rise time of about 300 nsec (700 G/μsec). For one set of experiments four probes were distributed around azimuthally. Since all four probes measure the same field perturbation and measure the same shape signal signature, similar to the one shown in

Fig. 3, it is taken as evidence that the plasma forms a complete ring. For these conditions, the peak of the poloidal field perturbation occurs at 1.7 μsec after the gun was triggered. This time corresponds to the gun acceleration time (between the plates, τ_{acc} = 0.8 μsec) plus the transit time (τ_{tr} = 0.9 μsec) at a constant velocity of 17 cm/μsec for arrival at the stopping point. This perturbation of the poloidal field falls off equally rapidly (approximately 700 G/μsec) to about one third the peak value. The subsequent rate of decrease (170 G/μsec) is about one fourth the initial rate. The equally rapid rise and fall of the field perturbation seems to indicate that the plasma boundary partially returns without dissipation whereas the subsequent slower decrease in field indicates some dissipative process may have occurred.

There is only a small signal reversal of about 5 percent (Fig. 3); if the plasma ring were to pass over the probe, a significant signal reversal would be expected. Such a reversal is observed for the case where the plasma ring velocity is 43 cm/μsec. This is consistent with the calculation of the stopping point in the poloidal field for this velocity without a flux conserving ring, which yields a required field larger than that produced to stop the plasma at the coils.

For the plasma travelling at 17 cm/μsec the ring arrives at the diagnostic beam placed at various radii as indicated in Fig. 4(a). For the positions R1, R2 and R3, (see Fig. 9), the sharp peak is the passage of the plasma ring ejected from the gun. At the position R4, the plasma ring arrives and dwells for a longer period, indicating that the outward travel of the ring has stopped. This is

verified by the measurement at position R5 where no significant line density is detected. The indication is that the outer stopping position lies between 33 cm and 35 cm. Comparing this stopping radius with the estimates from the stopping model (Eqn. 3 and Table I) suggests that the plasma ring must have spread laterally. Other possible variants to make the stopping model estimate agree would require a lower average velocity for the stopped particles or a lower number of particles.

The overall time evolution of the radial distribution of the line density (see Fig. 10) was constructed by using 16 traces of the time evolution of the line density at different radii. The dashed line indicates the outer position of the plasma ring which is observed to leave the gun at a reference time of 5μsec. The maximum radial position was attained at about 6μsec. The front returns at a reduced velocity (about 5 cm/μsec) and reaches an equilibrium position at 7μsec.

For the few experiments where the ring was expelled at 43 cm/μsec, the ring passage was observed for all measurable radii and the magnetic probe signal reverses, which indicates the passage of the plasma ring.

E. Plasma Confinement

The interferometer data give a picture of the radial line density distribution as shown in Fig. 10. After the outward travel, the plasma ring is stopped and reflected; an outer radial boundary of plasma at R = 30 cm appears to develop at about 7 μsec and remains stationary for the full duration of the measurement time, up

to 25 μsec. Since each position is based on only one discharge, it cannot be concluded that the outer boundary is as narrow as shown. An inner boundary is not distinctly discernible, possibly because of the build-up of density related to plasma coming from the gun after the initial ring ejection. An apparent inner boundary seems to be located between R = 24 and R = 26 cm, and is considerably broader than the outer boundary.

The line density build-up for late times (t > 12 μsec), within and at smaller radii than the inner boundary, is possibly due to neutral gas and plasma coming from the gun region. Some of the plasma build-up could be from subsequent cycles of the plasma gun as the stored energy from the capacitor bank rings down. The neutral gas would only register as it penetrates the inner boundary of the plasma ring and becomes ionized. After the 12 μsec time the build-up near the gun dominates the line density across the equilibrium region between R = 25 cm and R = 27 cm. The slowly increasing line density observed between R = 25 cm and about R = 27 cm could be due to neutral gas penetrating and diffusing in from the inner boundary or due to plasma trapped on field lines travelling around the equilibrium boundary (see Fig. 4) and out in radius to cross the interferometer line-of-sight. The basic signature of the line density is about the same between R = 26 cm and R = 30 cm except for the density build-up at times later than 13 μsec which is not observed for R = 27.7 cm.

The peak line density of 8×10^{15} cm^{-2} at R = 27.7 (Fig. 9) decays with a time constant of 15 μsec. At R = 30.5 cm, a much lower line density is observed for times after 7.5 μsec. The

measured line density before this time represents the passage and return of the outgoing plasma ring. For later times, the low line density is most likely due to the plasma passing through the cusp regions which extend through the line-of-sight of the interferometer.

The total number of particles trapped in the equilibrium region can be estimated from the radial distribution of line density $\langle n_e\, l_p \rangle$ between the inner and outer boundaries. Since the average peak $\langle n_e\, l_p \rangle$ between the boundaries is about constant at 6×10^{15} cm^{-2} (in Fig. 9 at R2, $\langle n_e\, l_p \rangle$ is slightly higher) the total particle number between R = 26 cm and R = 30 cm is $N_{eq} = 4 \times 10^{18}$. By comparison, the number of particles ejected from the gun during the first 0.5 μsec beginning at the rise of the burst (see the typical trace of Fig. 6) is between 3×10^{18} and 4.5×10^{18} depending on the discharge. This comparison between the gun ejected particle number (somewhat arbitrarily cut off) and the measured equilibrium number (depending on where the inner boundary is chosen between 24 and 26 cm) compare reasonably. Including the plasma up to an inner boundary of 24 cm would give a $N_{eq} = 5 \times 10^{18}$. Also, if the trailing particles after the burst were added to the equilibrium of this larger volume by taking the measured nl (Fig. 6) for an additional 0.6 μsec which is about the time between the ring stopping time and the time of the observance of an inner boundary (Fig. 7), then the total number ejected would be increased by 1.4×10^{18} particles. This addition would be an overestimate because the trailing particles would have a velocity smaller than 17 cm/μsec (i.e. they arrive later).

Thomson scattering data registered on three polychromater channels having a good signal-to-noise ratio (about 10:1) were taken at 7 μsec. The average obtained from 18 shots give an electron temperature of 15 eV with a standard deviation of 4 eV.

For different operating conditions (8 psia gas valve pressure instead of 7 psia) but with close to the same particle energy of the gun plasma, the scattering measurement gives 16 eV (average of 4 shots) at t = 7 μsec and 8 eV at t = 12 μsec. An estimate of the resultant decay time for the temperature is thus 7 μsec.

Taking the estimated particle number in the equilibrium position and assuming that the ions are also at 15 eV ($\tau_{ei} \simeq 3$ μsec), the initial energy content of the trapped plasma is 20 joules. Using the measured density and temperature decay times, the energy decay time is 5 μsec.

The measured final temperature is not much lower than that estimated by the shock model if the electrons and ions are assumed to be in equilibrium.

The plasma density, however, can only be estimated, based on the models which in part predict end conditions based on measured quantities. The stopping position measurement, compared with the predicted stopping position and combined with the shock model prediction, would suggest a final number density of 2.5×10^{14} cm^{-3} (Table I). The line density measurement of 6×10^{15} cm^{-2} for the final equilibrium combined with the plasma equilibrium shape calculation suggest a line-of-sight dimension of 11 cm at R = 28 cm which says the density is 5.5×10^{14} cm^{-3}.

Another way to estimate the density is to take the measured total number density between 26 cm and 30 cm as reported above and divide by the equilibrium plasma volume of 10^4 cm^{-3} calculated by the $\beta = 1$ model. The plasma density then is 4×10^{14} cm^{-3}.

The relative particle flux distribution along a line shown in Fig. 5(a) going across the field lines connected to the cusp region is shown in Fig. 11. The measured values are for three different conditions, all taken at 12 μsec after the plasma gun was triggered. The data give a distribution width of 2 to 3 ion gyro-radii, assuming the ions are 10 eV in temperature. These widths may be overestimated since the Faraday Cup showed evidence of saturation which would lower the peak and result in a larger half width than really exists. The location of the particle flux can be related back to the main body of plasma by following field lines. The width of the flux distribution, as measured to be about 2 to 3 ion gyro-radii in the poloidal field, is also about twice the boundary width (half on the inner and half on the outer boundary) of the equilibrium plasma, assuming flow along field lines. This corresponds to a 0.4 cm wide outer boundary and a 4 cm wide inner boundary, consistent with the plasma density data.

IV. CONCLUSIONS

Injection of the toroidally symmetric gun plasma into the bi-cusp field geometry has been achieved for the gun plasma velocity of 17 cm/μsec. The first step of the injection, that is stopping the expanding plasma ring, is observed by interferometry and

magnetic probes to be achieved with an outer limit of radial travel between 33 and 35 cm.

The model relating the stopping position to the ejected gun plasma ring indicates that the plasma ring must expand laterally in accordance with the acoustic velocity in order for it to be stopped at the measured position. The same diagnostics and model indicate that the gun plasma ring with a velocity of 43 cm/μsec is not stopped by the applied poloidal field. It remains to study this case with the use of a flux conserving barrier.

The second step, trapping the plasma in the magnetic well, is observed primarily by the interferometer measurement of a well defined outer boundary which remains stationary for the 20 μsec duration of the measurement. An inner boundary also seems to be in evidence although its definition is obscured by the plasma expelled from the gun after the initial burst. The measurements are not sufficiently detailed to ascertain the density gradient at the inner boundary. The indications given by the particle flux distribution emanating from the cusp region are that a sheath exists with a width of 1 to 1.5 ion gyroradii in the poloidal field. This distribution width is based on an ion temperature of 10 eV and assumes thermal equilibration of ions with electrons. Although this is not definitive evidence of a sheath structure, it is significant, especially since a sharp density gradient, one tenth the radial width of the plasma, is also measured at the outer boundary.

The total number of particles (4×10^{18}) measured between these two boundaries is comparable to the total number ejected from the gun in the initial burst, from 3×10^{18} to 4.5×10^{18}

particles. The plasma number density is uncertain with estimated bounds between 2.5×10^{14} and 6×10^{14} cm^{-3}.

The data give an electron temperature of 15 eV for the plasma which is expelled from the gun at a directed energy of 150 eV. Comparing the stopping time with the Alfven wave transit time suggests that a shock model is not entirely appropriate although the estimated electron temperature compares reasonably.

The plasma in the magnetic well is found to have a density decay time of 15 μsec, a temperature decay time of 7 μsec and, therefore, an energy decay time of 5 μsec. Estimates of particle flow out the cusp based on a width of two ion gyro radii give a density decay time of 25 μsec, i.e., of the same order as the measured time.

Overall, these results suggest that further work on the higher gun plasma energy with the addition of a flux conserving barrier may lead to higher temperatures for testing containment in TORMAC.

REFERENCES

BERKOWITZ, J., GRAD, H. RUBIN, H. 1958 Second U.N. Conference on Peaceful Use of Atomic Energy, Geneva, 31, 171.

BOOZER, A. H. LEVINE, M.A. 1973 Phys. Rev. Lett. 31, 1287.

BROWN, I. G., FEINBERG, B., KUNKEL, W.B., LEVINE, M.A., NILAND, R.A., SHAW, R.S., VAUCHER, B.G. 1982 Phys. Fluids 25, 79.

DE HOFFMAN, F. TELLER, E. 1950 Phys. Rev. 80, 692.

FEINBERG, B., NILAND, R. A., COONROD, J. LEVINE, M. A. 1983 "A 2-D Skin Current Toroidal-MHD-Equilibrium Code" LBL-10070.

GALLAGHER, C. C., COMBES, L. S., LEVINE, M. A. 1970 Phys. Fluids B, 1617.

GREENWALD, M. SMITH, W. I. B. 1977 Applied Optics 16, 587.

HAINES, M. G. 1977 Nuclear Fusion 17, 811.

JACKSON, J. D. 1962 "Classical Electrodynamics", Wiley.

LAWSON, J.D. 1957 Proc. Phys. Soc. Lond. B70, 6.

MYERS, B.R., LEVINE, M. A., PINCOSY, P. A. 1979 "A Toroidal Plasma Gun", LBL-9507.

MYERS, B.R., LEVINE, M. A., SHAW, R. S. 1981 Rev. Sci. Instr., 1187.

OSHER, J. E. 1962 Phys. Rev. Lett 8, 305.

SPALDING, I. 1971 Advances in Plasma Physics (ed. A. Simon and W. B. Thompson) John Wiley, New York 4, 79.

SPALDING, I. J., EDEN, M. J., PHELPS, A. D. R., ALLEN, T. K. 1969 "Theta-Cusp Containment", Plasma Physics and Controlled Nuclear Fusion Research, 2 IAEA, Vienna 639.

TIDMAN, D. A. KRALL, N. A. 1971 "Shock Waves in Collisionless Plasmas", Wiley-Interscience 14.

VELLA, M. C., FEINBERG, B., NILAND, R. 1979 "A Shock Heated Tormac Experiments", UCID-8095, LBL.

VLASES, G. C. 1967 Phys. Fluids 10, 2351.

WATTEAU, J.P.H. 1961 Phys. Fluids 4, 6076.

FIGURE CAPTIONS

Figure 1. Sectional view of the Tormac plasma gun and field coils. The gun supply was a 2 μf capacitor charged to 50 kV. The toroidal and poloidal fields were supplied by a 1.2 f electrolytic capacitor bank.

Figure 2. Vacuum field plot in the poloidal component. Note the relative positions of the poloidal coils and the gun plates.

[.] , [x] Poloidal field coils

Axial current 300 kAmp

a) Poloidal component of Ψ

Dashed line value 0.5×10^4 Gauss cm^2

Spacing between lines 1×10^4 Gauss cm^2

b) Contours of field magnitude: Note the magnetic well.

Dashed line value 2700 Gauss

Spacing between lines 183 Gauss

Figure 3. Plasma ring perturbation to the poloidal vacuum field during interaction with the poloidal field. Poloidal and toroidal fields plotted with radius. Data used for the stopping model equation are denoted.

Figure 4. Field plots a $\beta = 1$ plasma equilibrium is simulated by current loops (Δ) distributed on the boundary.

[.] , [x] Poloidal field coils

Axial current 300 kAmp.

a) Poloidal component of

Dashed line value 0.5×10^4 Gauss cm^2

Spacing between lines 1×10^4 Gauss cm^2

Note the positions of diagnostics

b) Contours of field magnitude

Dashed line value 2750 Gauss

Spacing between lines 500 Gauss

Figure 5. a) Field line plot of with the $\beta = 1$ simulated plasma which emphasizes the lines outside the toroidal and poloidal coil structures. Position of Faraday cup measurements is indicated.

Dashed line value 0 Gauss cm^2

Space between lines 1×10^4 Gauss cm^2

[.] , [x] Poloidal field coils

Axial current 300 kAmps

. . . . Additional flux lines at 0.5×10^4 spacing

b) Field lines plot of assuming that the plasma resides on vacuum field lines

Dashed line value -13.5×10^4 Gauss cm^2

Space between lines $2. \times 10^4$ Gauss cm^2

Figure 6. Measured line density temporal evolutions averaged over 16 discharges.

Figure 7. Particle number evolution averaged over 16 discharges.

Figure 8. Plasma arrival time referred to a plasma light emission peak as a function of position: A least squares fit to the data gives the velocity.

x Puff value pressure, 7 psig

Poloidal bank voltage 100 volts

o Modified gun

Figure 9. Line density temporal evolution taken at different radii. Those located as indicated in Fig. 4(a).

Figure 10. Evolution of the radial distribution of line density.

t = 5 μsec: plasma ring leaves the gun muzzle;

(R = 19 cm), V_p = 17 cm/μsec

t = 6 μsec: plasma ring reached the maximum radial travel;

(R = 34 cm).

t = 7 μsec: plasma ring returned to R = 30, V_f = 5 cm/μsec

The dashed line follows the outer boundary location.

Figure 11. Relative particle flux distribution across field lines connected to the cusp field. Note ref. [Fig. 4(b)] the relative length of an ion gyro radius if T_2 = 10 ev.

O 8 psia; 3470 μsec valve timing

Δ 8 psia; 3500 μsec

7 psia; 3470 μsec

Table 1 : SHOCK MODEL PARAMETERS

Number Density n_e (cm^{-3})	1×10^{15}	5×10^{14}	2.5×10^{14}
Lateral Width a (cm)	3	6	12
(Equation 3) Stopping Position R_2 (cm)	39.4	37.2	35.4
(Equations 6-13) Initial Beta	0.14	0.07	0.035
Plasma Ring Mach No. M_p	1.45	1.02	0.72
Shock Mach No. M_1	2.5	2	1.7
Post Shock Temperature T_2 (eV)	75	61	49
Final Temperature $T_f = T_i + T_e$	38	37	34
Final Density n_f (cm^{-3})	9×10^{14}	5×10^{14}	2.5×10^{14}
Final Beta β_f	0.34	0.19	0.09

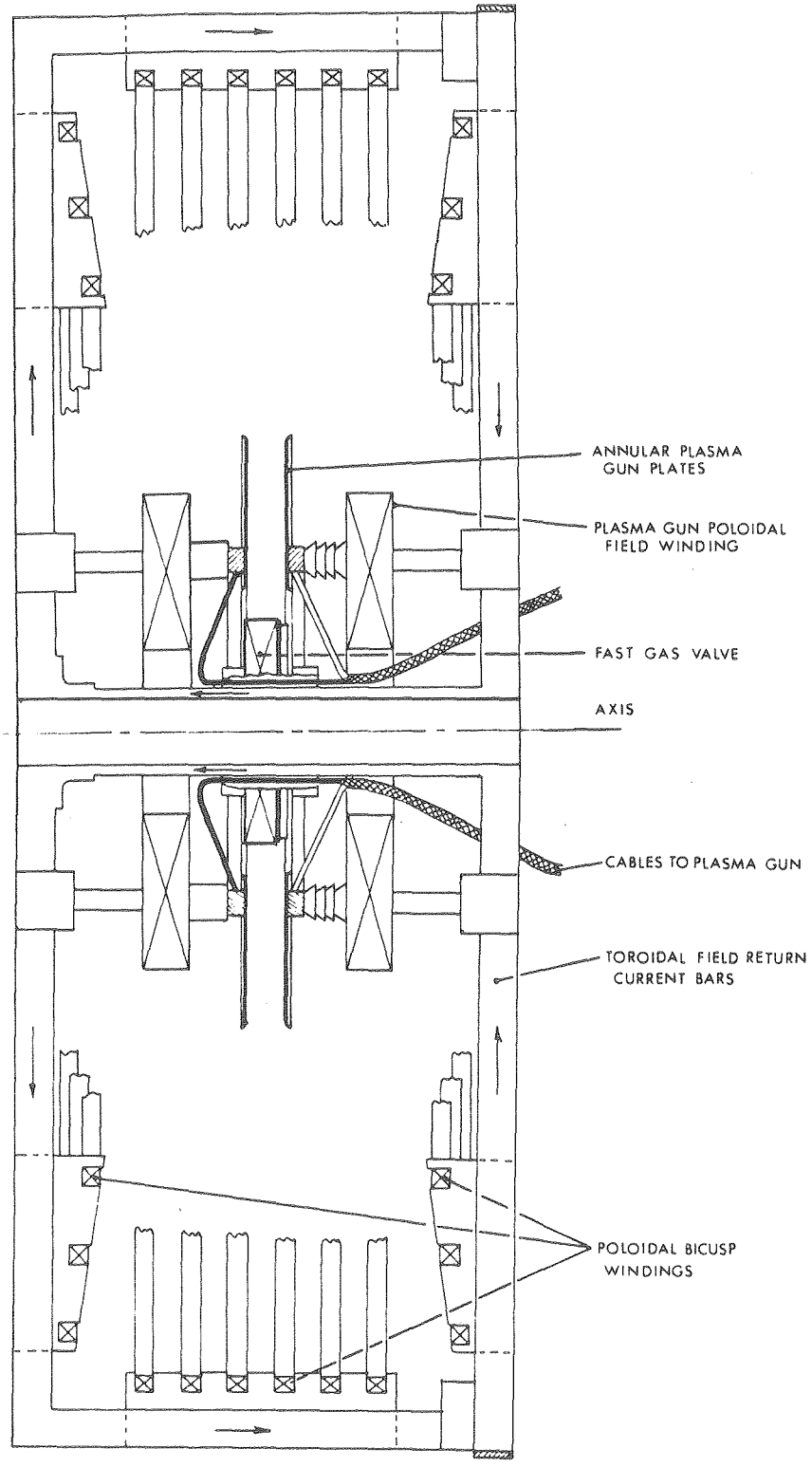

XBL 798-10923

Fig. 1

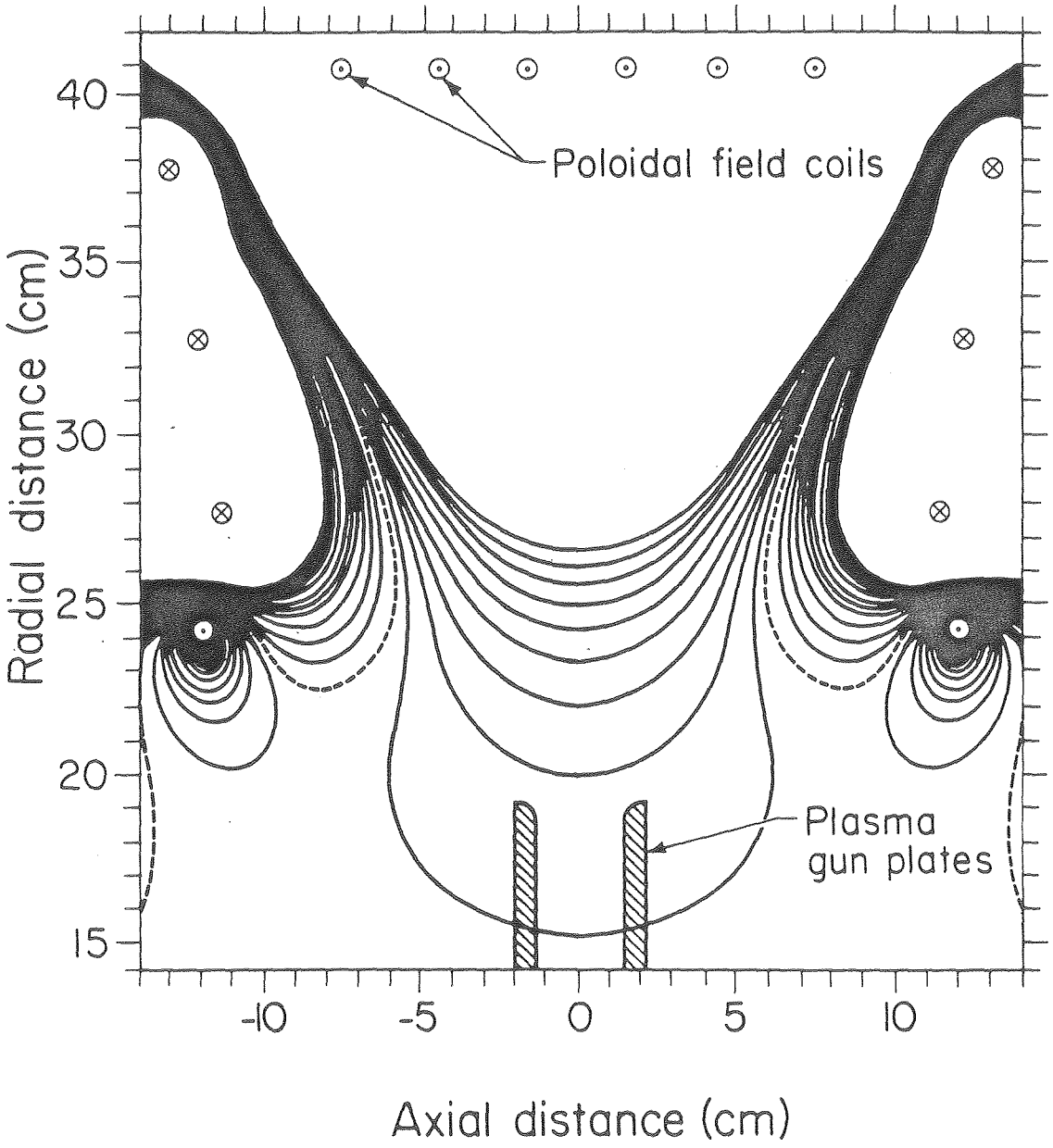

Fig. 2a

XBL 8010 - 2213

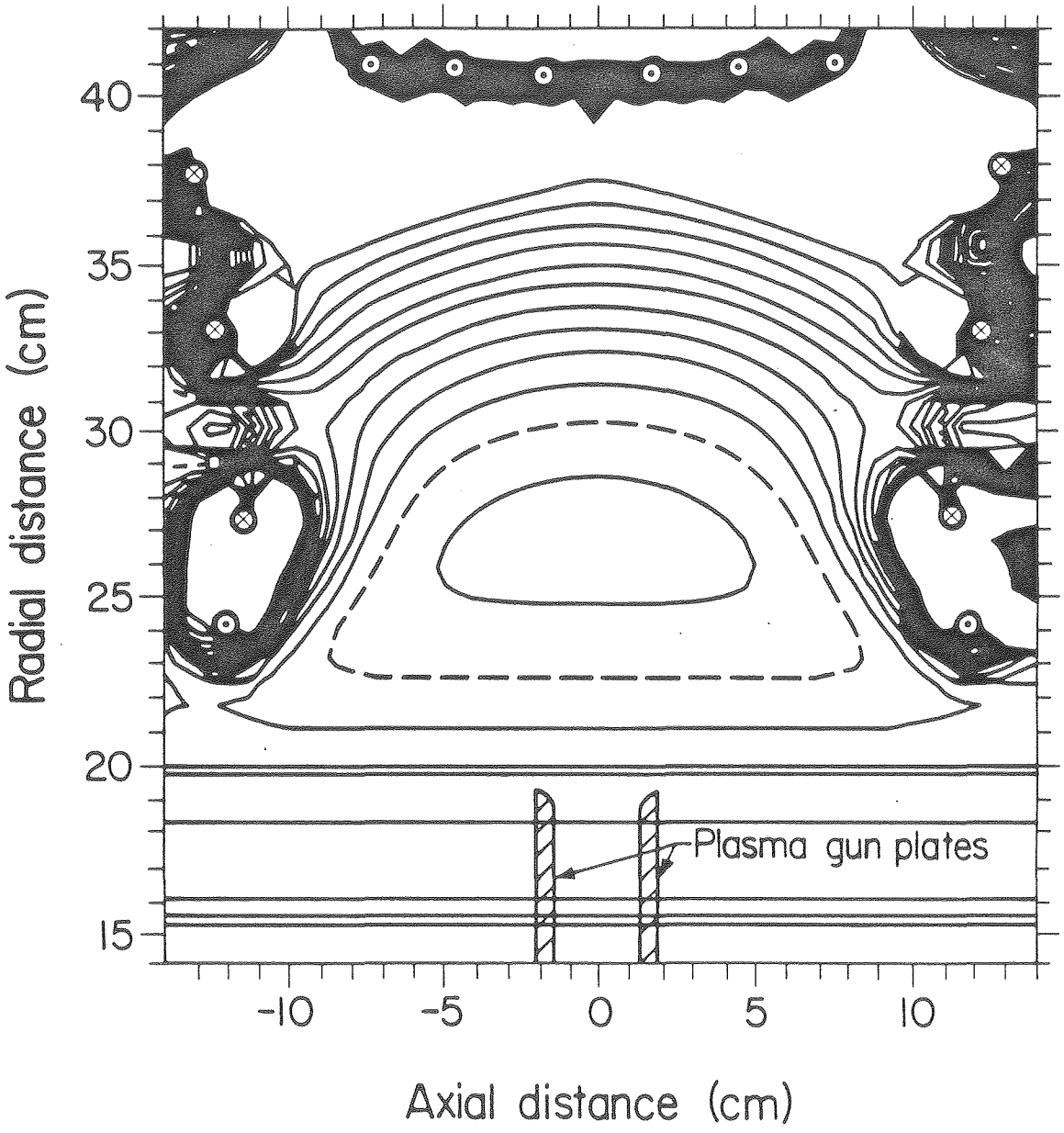

XBL 8010-2216

Fig. 2b.

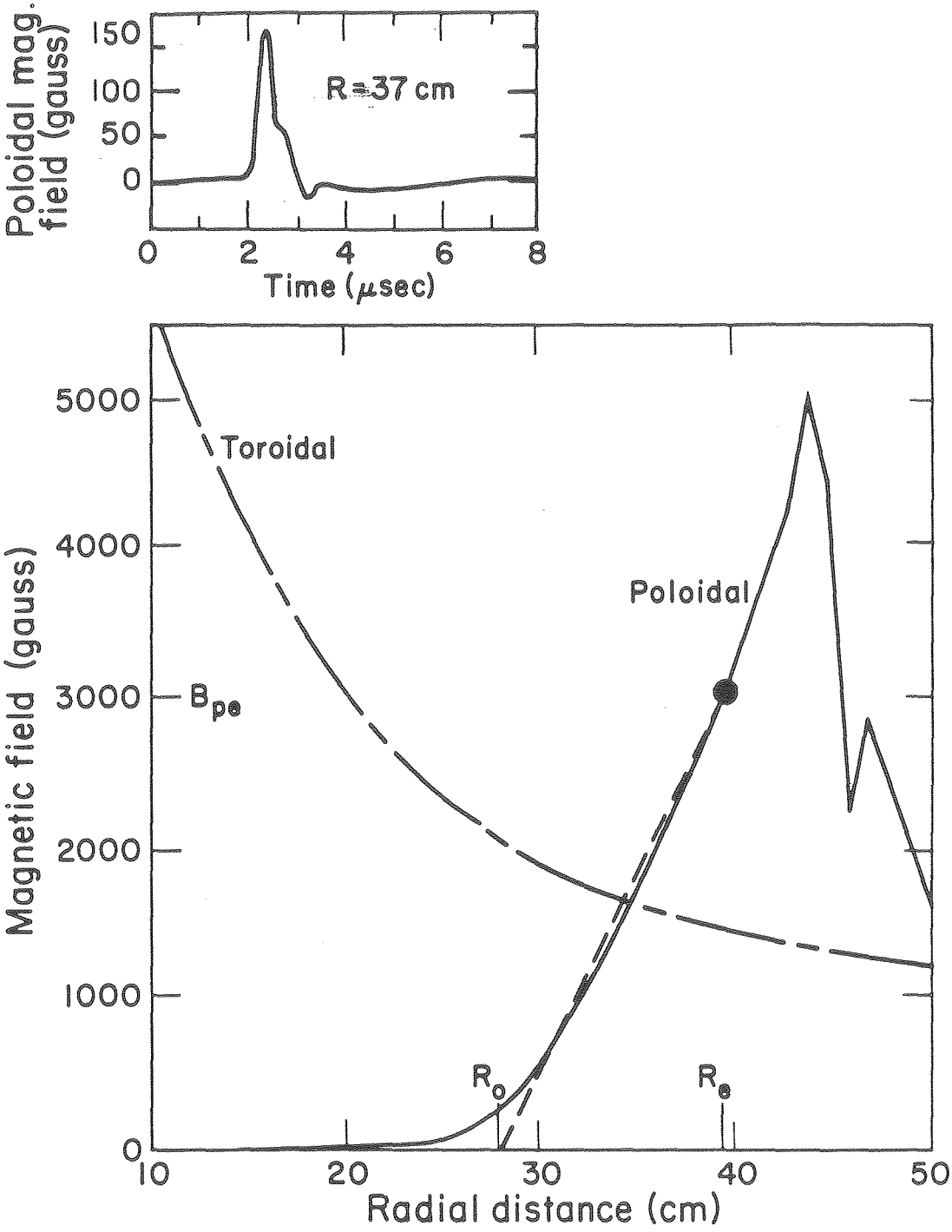

Fig. 3

XBL 8010-2211

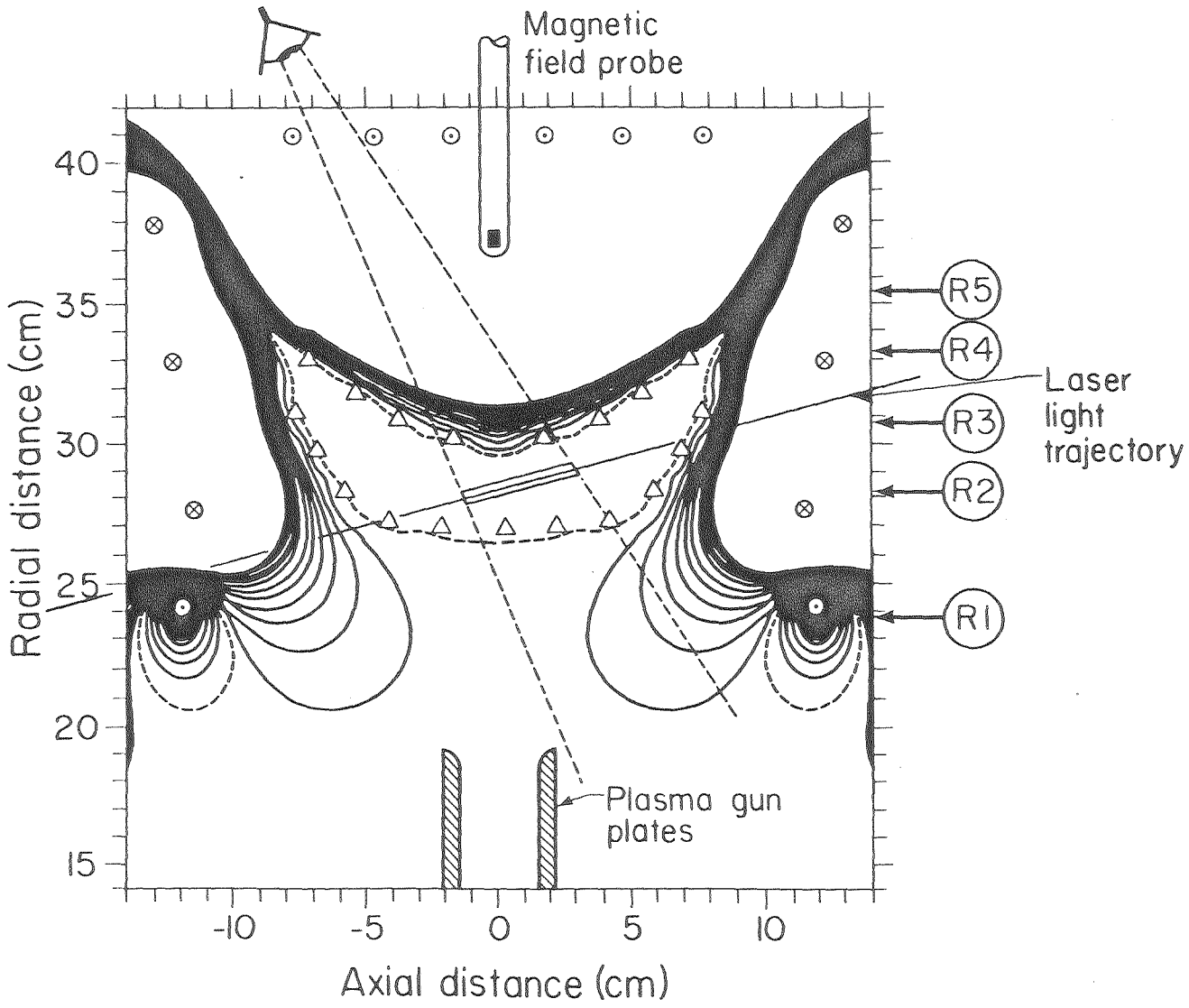

Fig. 4a

XBL 8010 - 2215

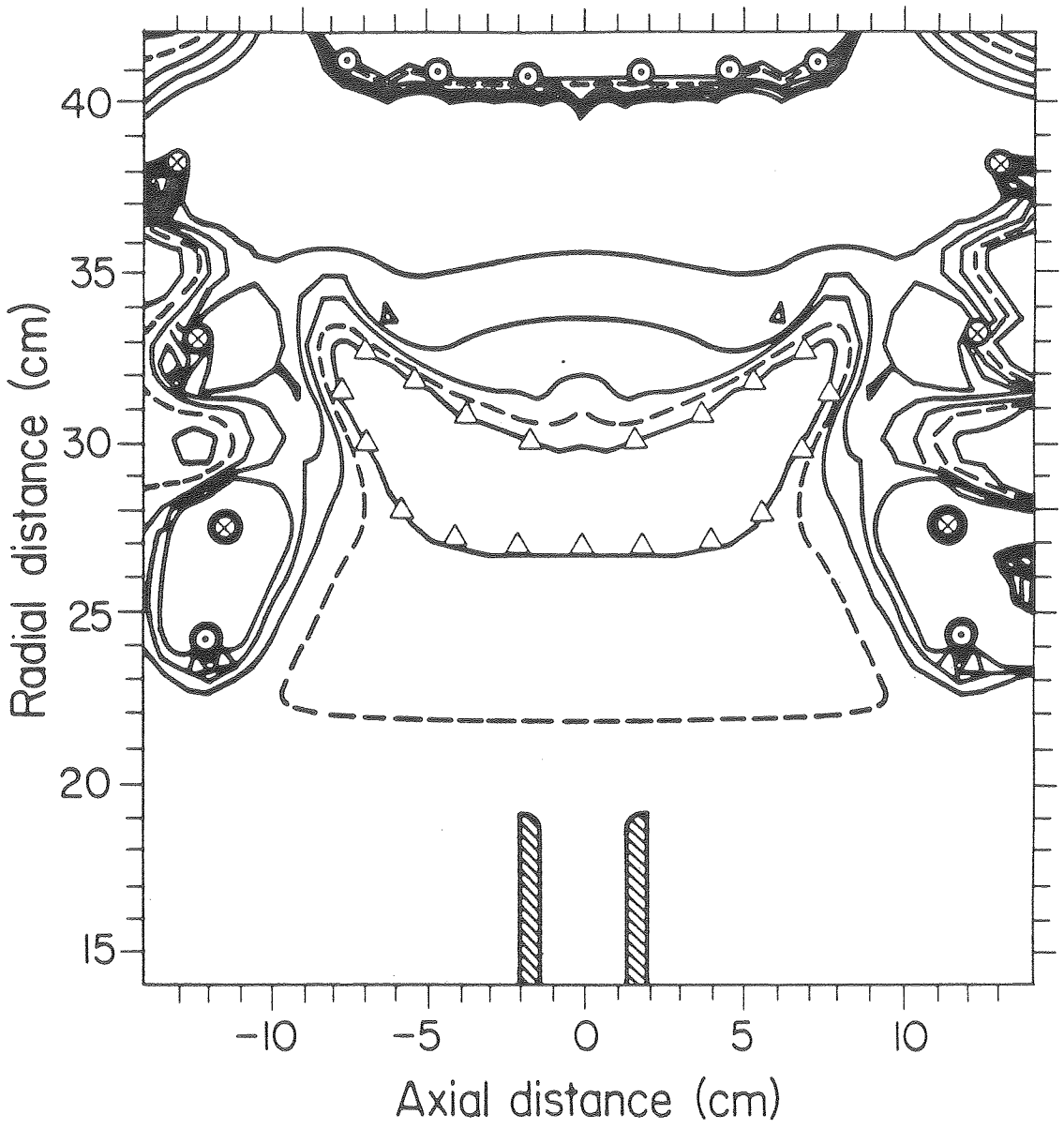

Fig. 4b.

XBL 8010-2214

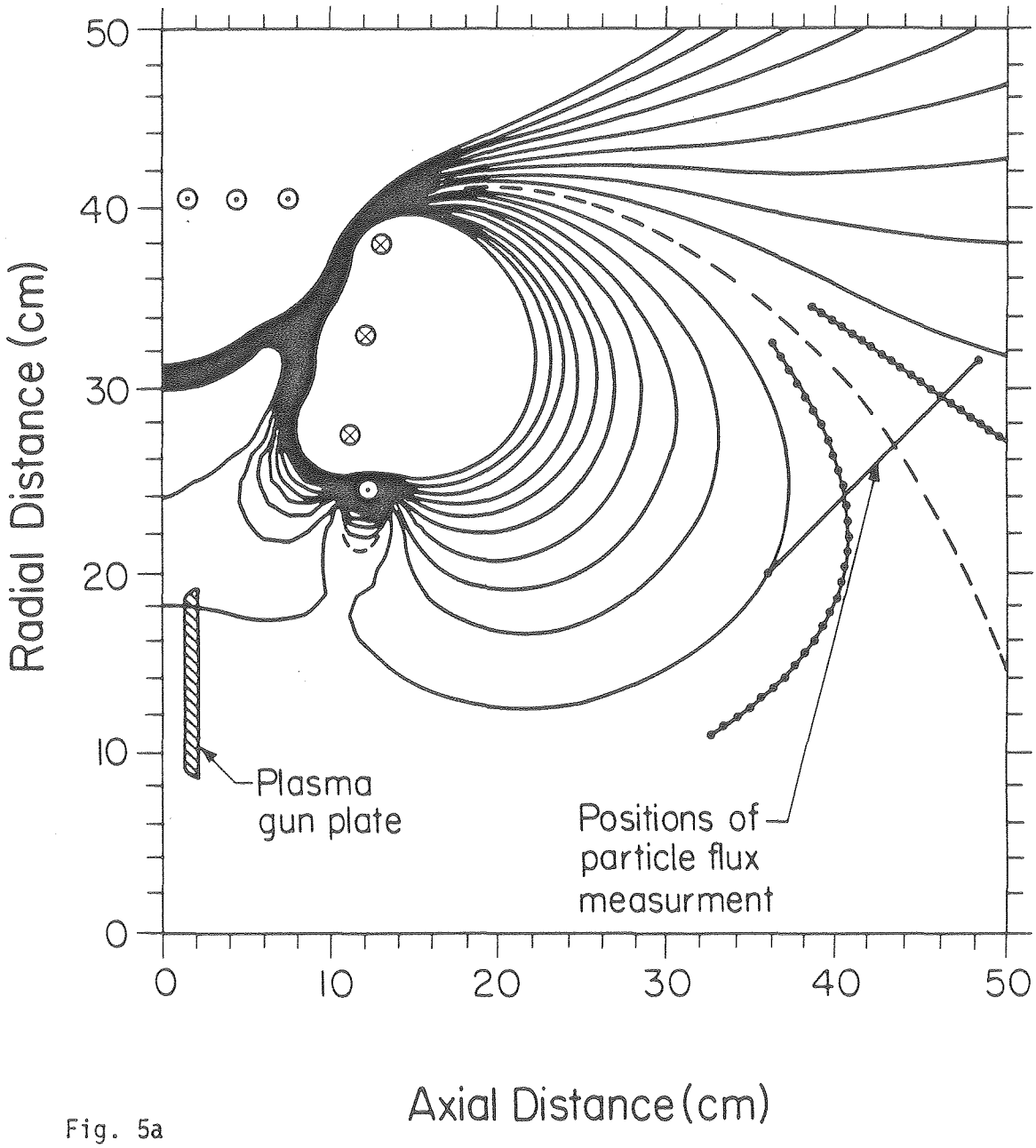

Fig. 5a

XBL 8010-2219

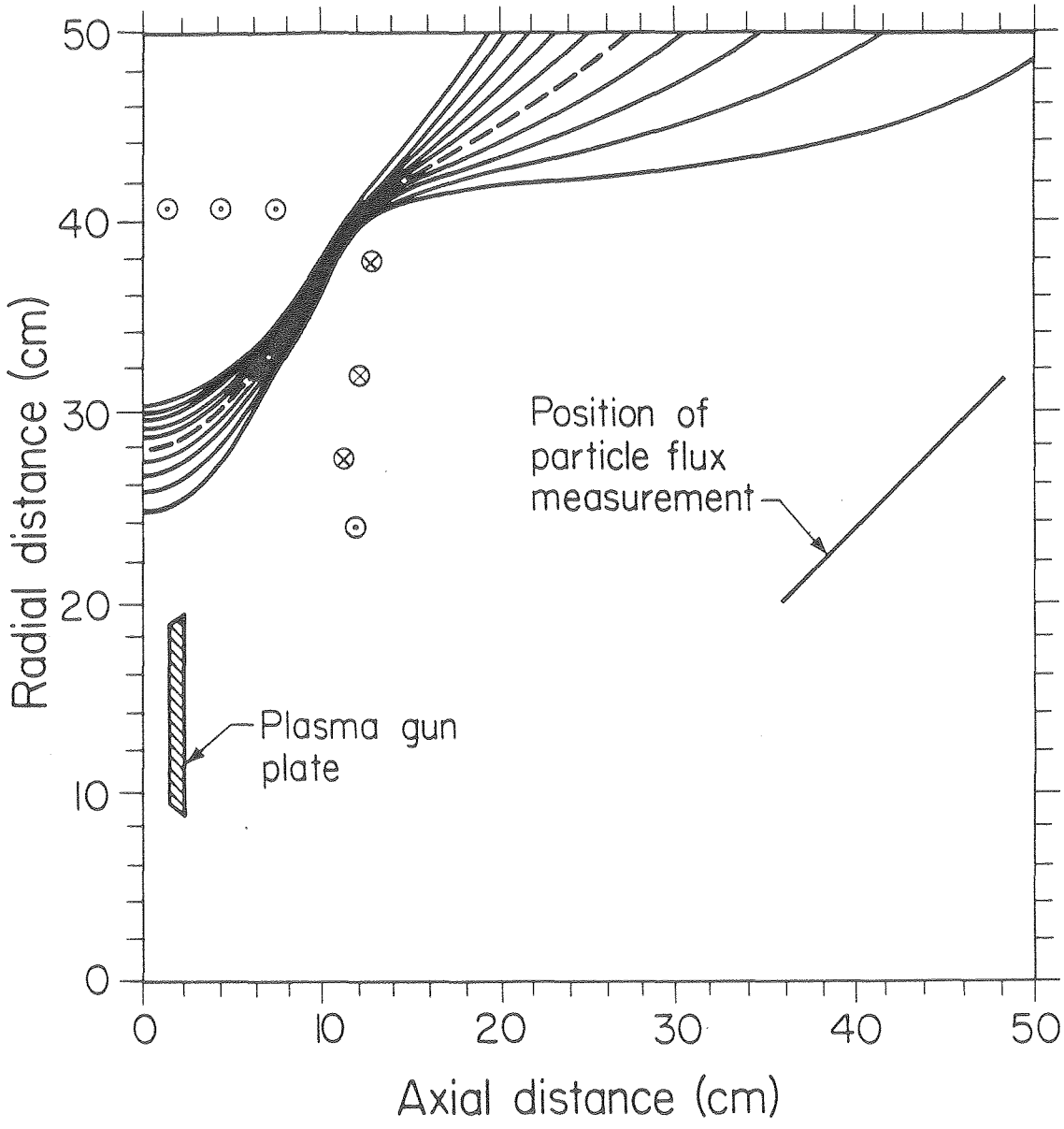

Fig. 5b

XBL 8010-2020

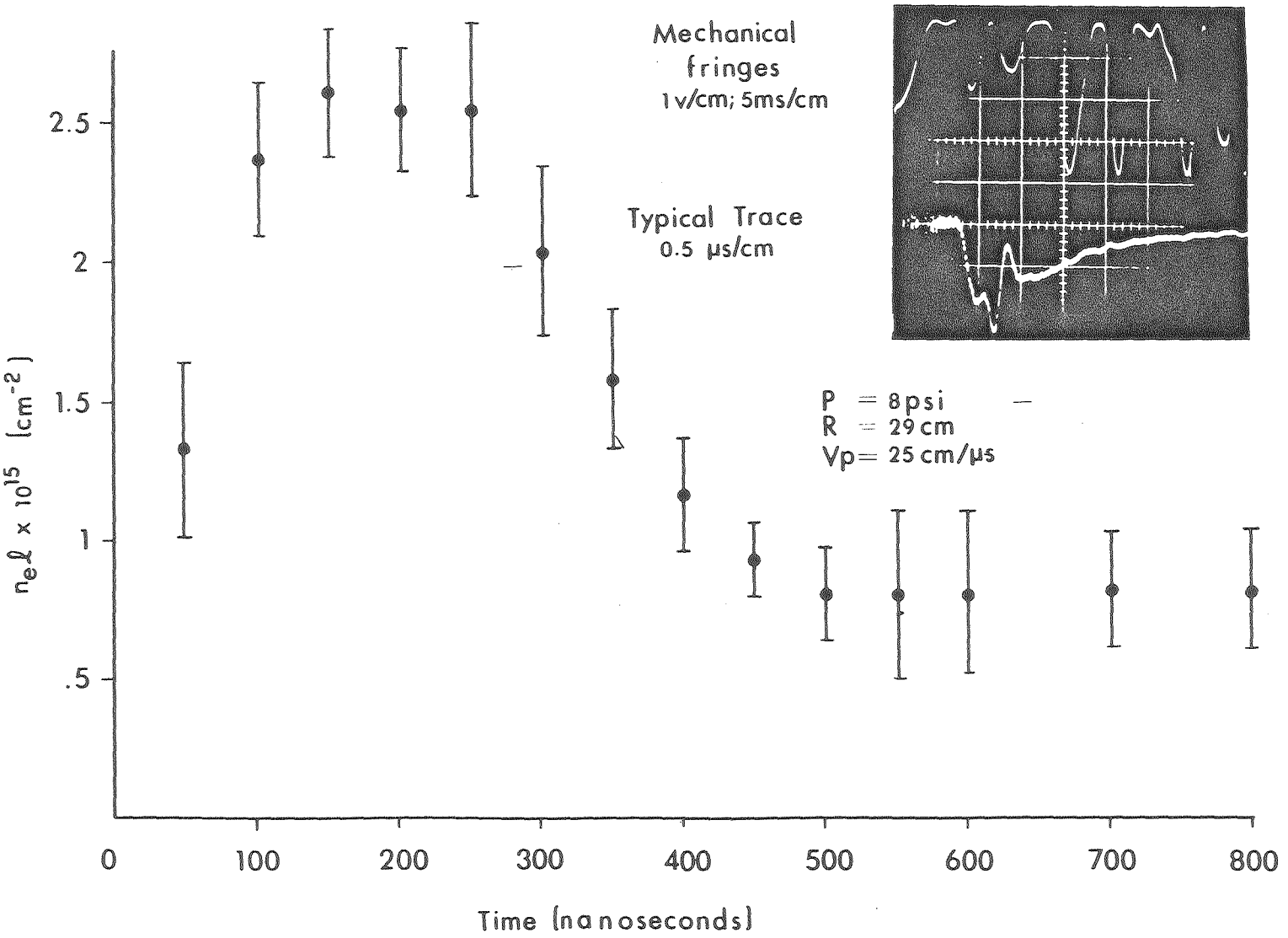

Fig. 6

XBB 801-94

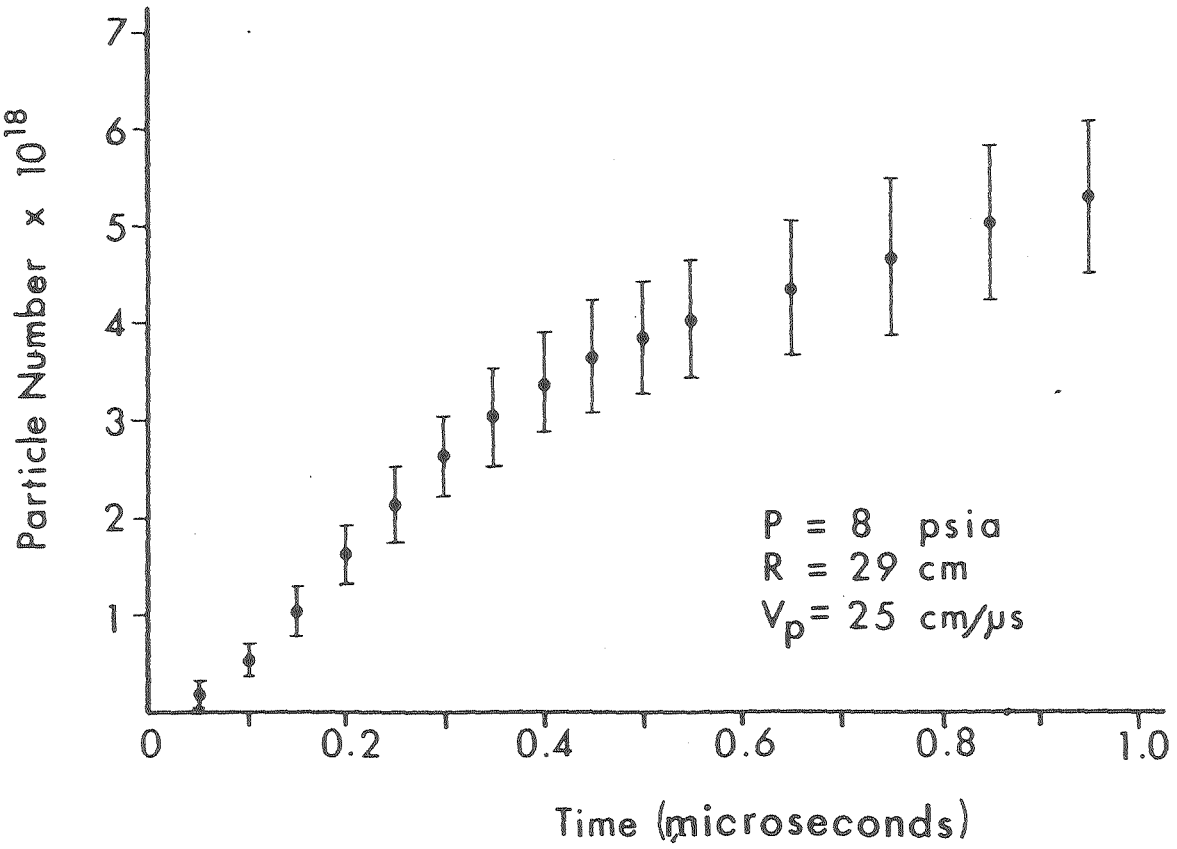

Fig. 7

XBL 801-7611

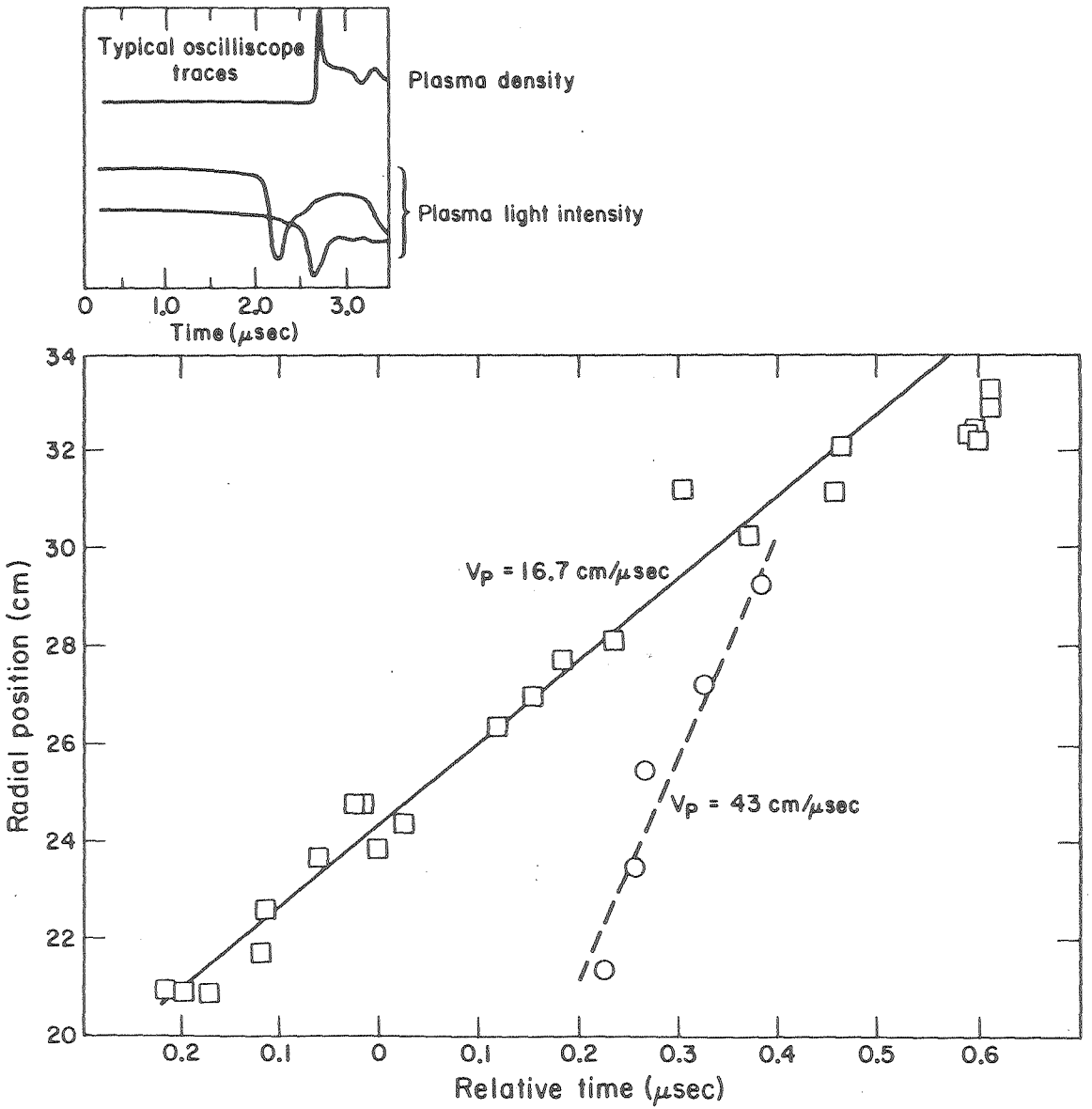

Fig. 8

XBL 8010-2217

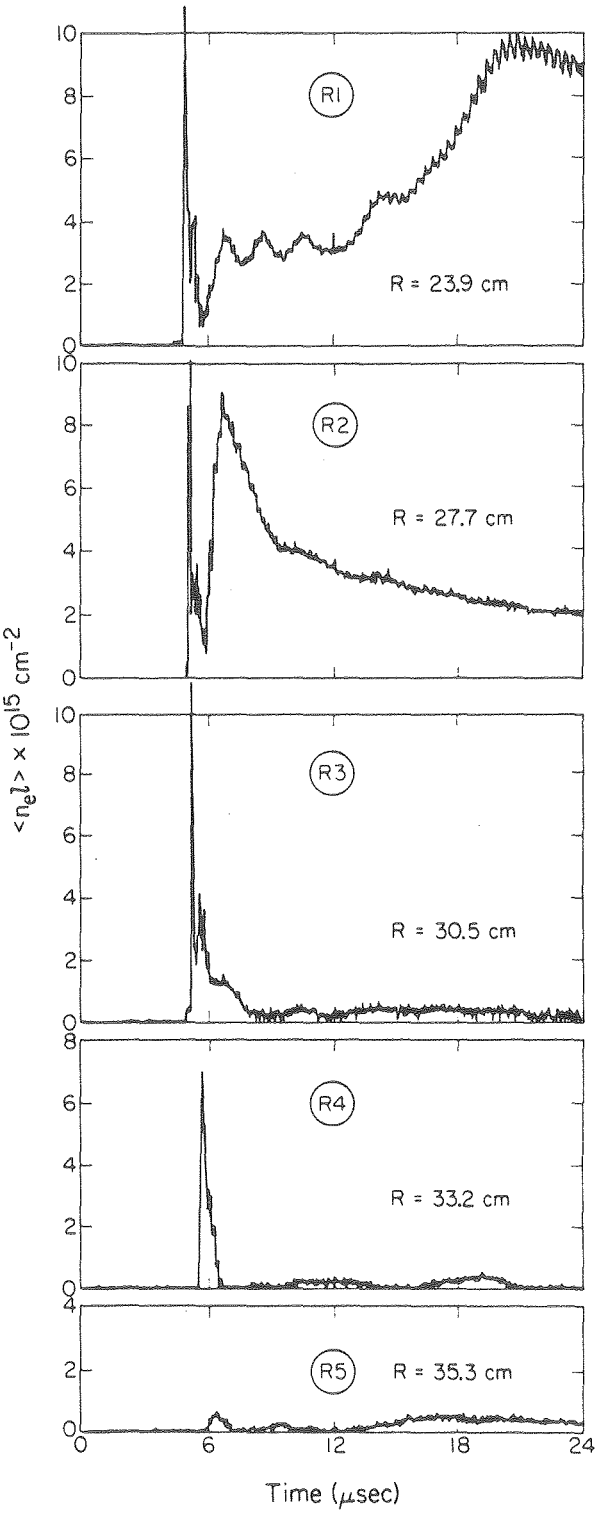

Fig. 9

XBL 8010-2218

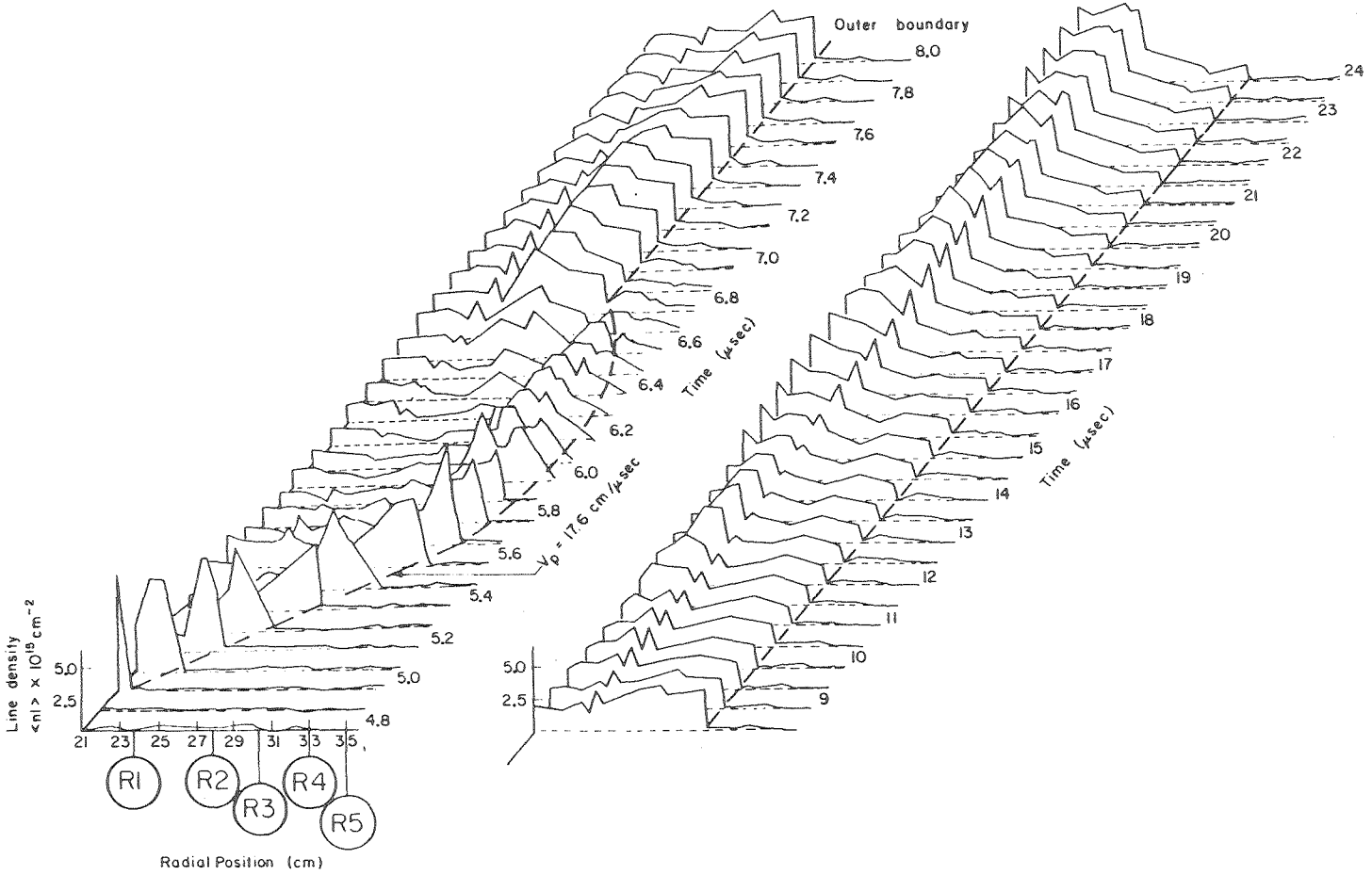

Fig. 10

XBL 8010-2221

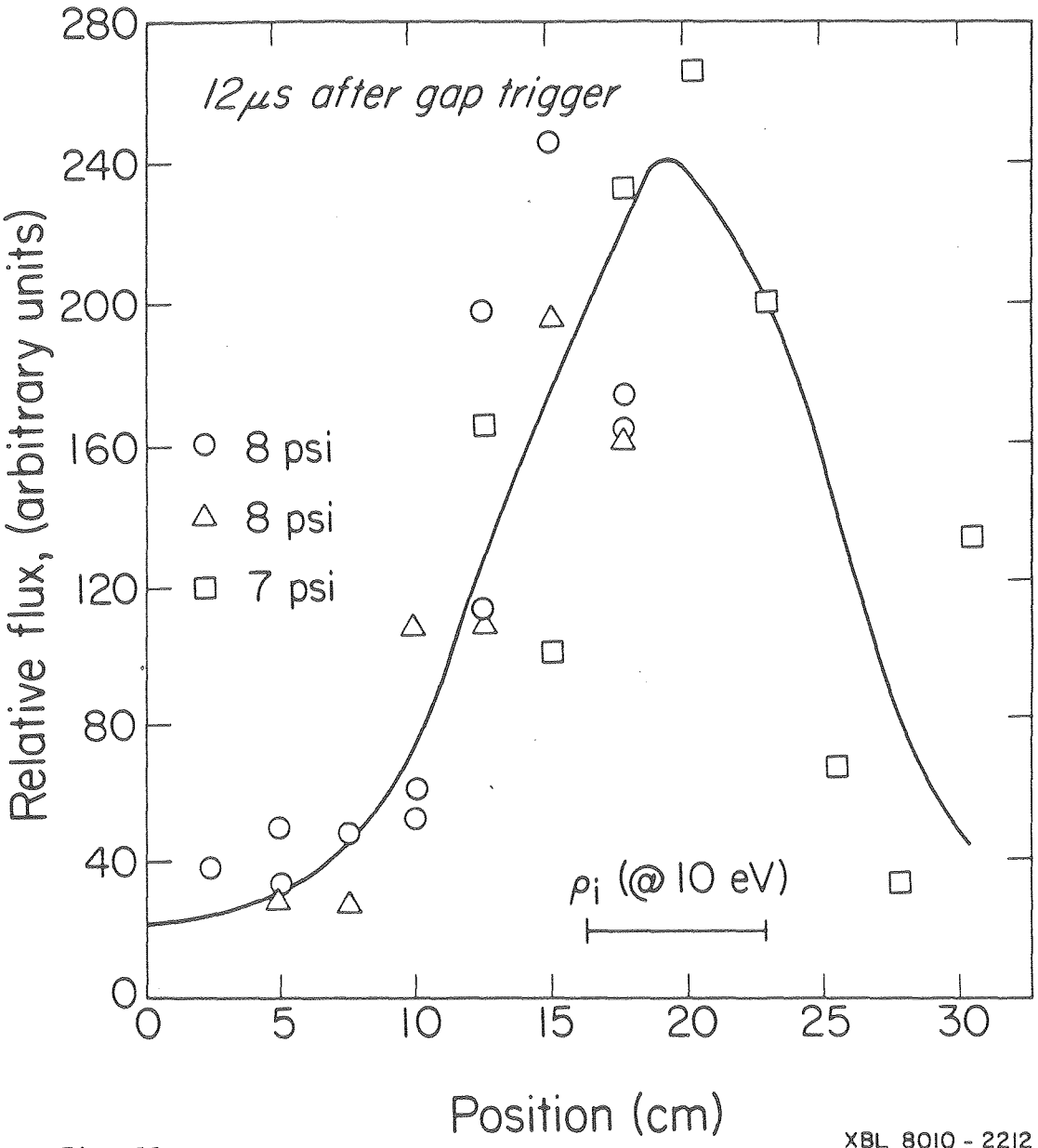

Fig. 11

XBL 8010 - 2212